Detection and discrimination between oil spills and look-alike phenomena through neural networks

K. Topouzelis [a,*], V. Karathanassi [b], P. Pavlakis [c], D. Rokos [b]

[a] Joint Research Centre — E.C., Institute for the Protection and Security of the Citizen, Sensors, Radar Technologies and Cybersecurity Unit, Italy
[b] Laboratory of Remote Sensing, School of Rural and Surveying Engineering, National Technical University of Athens, Heroon Polytechniou 9, GR-15780, Greece
[c] Hellenic Centre for Marine Research, Greece

Abstract

Synthetic Aperture Radar (SAR) images are extensively used for dark formation detection in the marine environment, as their recording is independent of clouds and weather. Dark formations can be caused by man made actions (e.g. oil spill discharging) or natural ocean phenomena (e.g. natural slicks, wind front areas). Radar backscatter values for oil spills are very similar to backscatter values for very calm sea areas and other ocean phenomena because they damp the capillary and short gravity sea waves.

The ability of neural networks to detect dark formations in high resolution SAR images and to discriminate oil spills from look-alike phenomena simultaneously was examined. Two different neural networks are used; one to detect dark formations and the second one to perform a classification to oil spills or look-alikes. The proposed method is very promising in detecting dark formations and discriminating oil spills from look-alikes as it detects with an overall accuracy of 94% the dark formations and discriminate correctly 89% of examined cases.

1. Introduction

Several man made and natural ocean phenomena dampen the wind generated short gravity-capillary waves which are the primary backscatter agents of the radar signals. For this reason, some areas appear dark on SAR imagery in contrast to the surrounding sea. Any area on an image which is sufficiently darker than the neighbouring area can be characterized as a dark formation. Nevertheless, even in a single image, the degree of darkness and contrast required for the dark areas characterization is not constant due to SAR image complexity (e.g. different backscattering values from near and far range), to different sea states and to different dark formation characteristics. It is particularly hard to determine how much darker an area has to be and there is no sufficient answer in literature. Dark formations can be (Alpers et al., 1991; Hovland et al., 1994): oil spills, low wind areas,

* Corresponding author. Tel.: +39 0332789609.
  E-mail addresses: Kostas.Topouzelis@jrc.it (K. Topouzelis), karathan@survey.ntua.gr (V. Karathanassi), ppavla@ncmr.gr (P. Pavlakis), rslab@survey.ntua.gr (D. Rokos).

organic film, wind front areas, areas sheltered by land, rain cells, current shear zones, grease ice, internal waves and upwelling zones.

Traditionally, the detection of dark formations constitutes the first step in oil spill detection approaches (Martinez and Moreno, 1996; Ziemke, 1996; Kubat et al., 1998; Benelli and Garzelli, 1999; Lu et al., 1999; Solberg et al., 1999; Del Frate et al., 2000; Gade et al., 2000; Keramitsoglou et al., 2002; Topouzelis et al., 2002). When dark formations are detected, statistical classification methods are applied to characterize them as oil spills or look-alike objects. Mainly dark formations are located manually by cropping a broader area containing the dark formation (Calabressi et al., 1999; Del Frate et al., 2000; Lichtenegger et al., 2000). An image window with fixed size can be used, in which threshold algorithms — adapted or not — can be used (Solberg and Theophilopoulos, 1997; Solberg et al., 1999). In more sophisticated studies, the image window does not have fixed size but can vary according to brightness and contrast values (Karathanassi et al., 2006). The last technique takes advantage of the different contrast and intensity values which are contained in a single SAR image and detects dark areas with various brightness values located in different sea-state environments. All the above studies use statistical based techniques to locate dark formations. They many times fail to detect dark formations correctly because of non-linearly separable datasets introduced in the statistically-based decisions. The pixel values of a dark area and its surroundings are not following a linear distribution due to radar complexity (e.g. noise, differences because of near and far range). This is the reason why a simple threshold cannot distinguish dark formations from clean sea in a single SAR image and more advanced, i.e. adaptive thresholds, have to be used.

Recent work has demonstrated that NNs represent an efficient tool for modelling a variety of non-linear discriminant problems. NNs may be viewed as a mathematical model composed of several non-linear computational elements called neurons, operating in parallel and massively connected by links characterized by different weights (Bishop, 1995; Ziemke, 1996; Kanellopoulos and Wilkinson, 1997; Del Frate et al., 2000). Artificial NNs can be used in order to learn and reproduce rules or operations from given examples. NNs have been successfully used for remote sensing applications (Bishop, 1995; Kanellopoulos and Wilkinson, 1997; Del Frate et al., 2000; Kavzoglu and Mather, 2003). NNs have been used to detect dark formations by Topouzelis et al. (2006), to classify a dark formation as oil spill or look-alike in SLAR images by Ziemke (1996), and in SAR

images by Del Frate et al. (2000), Topouzelis et al. (2003), Topouzelis et al. (2004). To our knowledge, the combination of both dark formation detection and oil spill and look-alike discrimination by neural networks is not reported in the literature. This paper investigates the potential of the neural networks to detect dark formations and to discriminate oil spills and look-alikes simultaneously.

The paper is organized in five sections. In Section 2 the used dataset is described and in Section 3 the proposed methodology is given. Results and conclusions follow in Sections 4 and 5, respectively.

2. Data

Most of the oil spill detection studies use low resolution SAR data (quick-looks) with nominal spatial resolution of 100 m × 100 m to detect oil spills (Solberg and Theophilopoulos, 1997; Espedal and Wahl, 1999; Solberg et al., 1999; Fiscella et al., 2000; Espedal and Johannessen, 2000; Pavlakis et al., 2001; Brekke and Solberg, 2005). Low resolution data are sufficient for large scale monitoring but small and fresh spills cannot be detected sufficiently as they are represented in very few pixels and because they present brighter contrast than the bigger and older oil spills. For the present study a dataset of 24 high resolution SAR images with spatial resolution of 25 m × 25 m was used in order to evaluate the proposed methodology. The dataset contains several sea states, all images contain several dark objects and have been used previously by different studies (Pavlakis, 2001; Pavlakis et al., 2001). Example of oil spills and look-alikes can be seen in Fig. 2. The processing time for an image window of 4–16 Mb size from a European Remote Sensing satellite 2 (ERS-2) scene is 2–5 min. The method was applied on image windows of 4–16 Mb rather than complete scenes to speed up the process and to test its performance in terms of time requirements and result quality. From the above 24 SAR images 159 image windows are extracted containing 90 look-alikes and 69 oil spills. The classification of dark signatures made by photointerpretation and the size of the extracted widows varies according to the size of the dark features. We randomly split the available data set into equally sized parts to use one for training and the other for testing in the neural network classification. Both sets contain an almost equal number of look-alikes and oil spills.

A pre-processing phase was needed to prepare the image windows for classification. Preparing the data includes filtering and data normalization. Filtering an original SAR image has a double aim: first to remove image speckle and second to smooth the image values. Attempts to use unfiltered images for dark feature

detection failed. A combination of the Lee and Local Region filters has proved to be appropriate (Rio and Lozano-García, 2000; Topouzelis et al., 2006). Following filtering, image values were transformed into certain interval values i.e., they were normalized. Normalization is important for neural network in order to ensure that the distance measure responses with equal weight for each input. Without this procedure any input unit with large value will dominate the results. Normalization was performed with linear transformation from the image interval [0–255] to neural network interval [0–1]. It is of high importance to use the 256 grey values as image interval and not the values coming from the minimum and maximum of each window. Otherwise, the final classification would be biased and the generalization would fail.

3. Method

A methodology using two neural networks, one to detect dark formations and one to classify them is developed (see Fig. 1). The first neural network uses as input SAR images (pixel intensity values) and produces a black–white image with the detected dark formations. These dark formations can be seen as a group of black pixels forming dark objects. For each detected dark

Fig. 1. Flow diagram of the proposed method.

object a set of 10 features was calculated. These features were used as input to the second neural network, which decides if the dark formation is an oil spill or not.

3.1. Dark formation detection

The network used for dark formation detection was a fully connected feedforward with 1:3:1 topology. This network was selected as the one with the highest accuracy in dark formation detection (Topouzelis et al., in press). Pixel intensity values were used as inputs to the neural network. The input values were modified to fit correctly to neural networks during the pre-processing stage. Small areas of the above mentioned training set were chosen. For each image window two very small training areas were selected: one presenting dark formation and one presenting sea. The neural network used is a standard fully connected feedforward multilayer perceptron trained by the standard backpropagation algorithm (Rumelhart and McClelland, 1986). A Log sigmoid transfer function is used and we set learning rate to 0.05, momentum to 0.9 and the maximum number of epochs to complete to 500. The neural network is trained with the backpropagation variant using the training set. The efficiency of the proposed network was examined using the testing set with the set of weights discovered during training. For each test data, a two bit (black and white) image containing the dark area and the surrounding sea was produced.

For each image produced by neural networks a comparison with a reference dataset was made. The reference dataset was produced by the authors using photointerpretation methods and techniques. The comparison was made using confusion matrices. For each produced image, the overall, dark formation and sea accuracy was calculated through the confusion matrix. Overall accuracy was calculated by dividing the total number of the pixels correctly classified by the total number of the pixels of the sample. Dark formation accuracy was calculated by dividing the number of pixels correctly classified as dark area by the total number of the pixels referenced as dark area. Sea accuracy was calculated similar to dark formation accuracy, taking into account the total number of pixels referenced as sea area.

Overall and sea accuracies were expected to present quite high values as the reference dataset mainly includes large sea areas. Sea discrimination is not the main task of the presented work; however, it is very crucial in order to detect dark formations correctly. Low sea accuracy mainly represents dark formations which
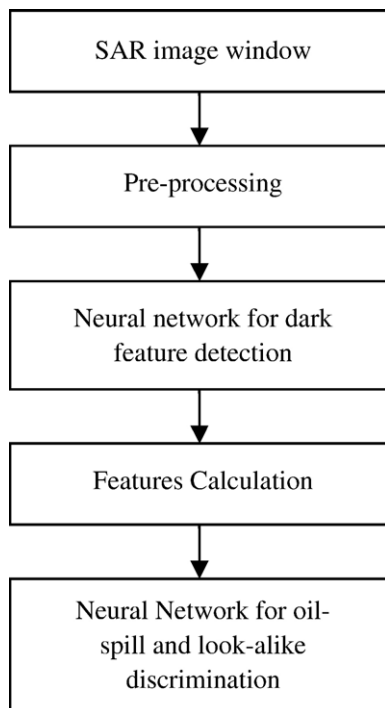
do not exist in reality and they can be considered as image noise. Dark formation accuracy had great importance as the number of pixels presenting dark formations was much smaller than those representing the sea. The networks' performance is described in the next section of the paper.

3.2. Dark formation discrimination between oil spills and look-alikes

After the dark formation detection by the first neural network, a second one was responsible to discriminate between oil spills and look-alike. In this case input data were not pixel values but a vector of 10 features which has proved to be optimum for oil spill and look-alike discrimination (Stathakis et al., 2006). Using the two bit (black and white) image, from the dark formation detection, a raster to vector conversion was applied in order to transport the dark formation to vector and to calculate the 10 features. This second network and the selected inputs were chosen using a genetic algorithm. The genetic algorithm had chosen the selected 10 from a base of 25 inputs and the proper topology after searching 100 generations using 7 bit chromosome. Detailed information regarding the selected topology and the feature selection is given by Stathakis et al. (2006).

In details the features that are used to discriminate between oil spills and look-alikes are:

1. Perimeter to area ratio (P/A): The ratio between the perimeter (P) and the area (A) of the object.
2. Object Complexity (C): Describes how simple (or complex) the geometrical objects are (Del Frate et al., 2000; Solberg et al., 1999; Karathanassi et al., 2006). Here it is defined as the border length e of the image object divided by four times the square root of its area A $\left(C = \frac{e}{4\sqrt{A}} \right)$.
3. Shape factor (SP): Describes the general shape of the object. It is referred to as "first invariant planar moment" in Solberg et al. (1999), as "form factor" in Fiscella et al. (2000) and as "asymmetry" in Topouzelis et al. (2002). Here the "asymmetry" is chosen computing the ratio of the lengths of minor and major axes of an ellipse describing the object shape.
4. Object standard deviation (OSd): Standard deviation of the intensity values of the pixels belonging to the oil spill candidate.
5. Object power to mean ratio (Opm): The ratio between the standard deviation (OSd) and the mean (OMe) values of the object.

6. Background standard deviation (BSd): Standard deviation of the pixels intensity values of an area surrounding the object (approximately double of the pixels forming the dark area).
7. Ratio of the power to mean ratios (Opm/Bpm): The ratio between the object power to mean ratio (Opm) and the background power to mean ratio (Bpm).
8. Local area contrast ratio (ConLa): The ratio between the mean backscatter value of the object (OMe) and the mean backscatter value of an area surrounding the object (approximately double of the pixels forming the dark area).
9. Mean border gradient (GMe): It is the mean of the magnitude of gradient values of the region border area. The Sobel operator is used to compute the gradients.
10. Mean Haralick texture (THm): It refers to the mean Haralick (1979) texture based on sub-objects. It is calculated as the average of the grey level co-occurrence matrices of the sub objects.

The feature values were again transformed to neural networks internal [0–1] in order not to be biased. The second network had a 10:51:2 topology. This was selected as the most effective one (Stathakis et al., 2006). The neural network used is a standard fully connected feedforward multi-layer perceptron trained by the backpropagation algorithm (Rumelhart and McClelland, 1986). A Log sigmoid transfer function is used and we set learning rate to 0.03, momentum to 0.9 and the maximum number of epochs to complete is 110. The neural network is trained with the backpropagation variant using the training set of 45 look-alikes and 35 oil spills. The test set is then classified using the set of weights previously discovered. Note that in this phase the operation is done on objects rather than pixels.

All the necessary steps concerning neural networks (creation, training and results production) were made using the Stuttgart Neural Network Simulator (SNNS) v4.2 software. Where necessary, (e.g. for pre-processing and feature calculation) ancillary programs were created using the IDL v6.1 language.

4. Results

In general, the results show that the method presented here is very efficient in detecting dark formations and discriminating oil spills from look-alikes. Regarding dark formation detection the mean overall accuracy for the testing data was 94%, the mean dark accuracy was 91% and the mean sea accuracy was 95%.

a) Detection of a well-defined old oil spill on a dark background
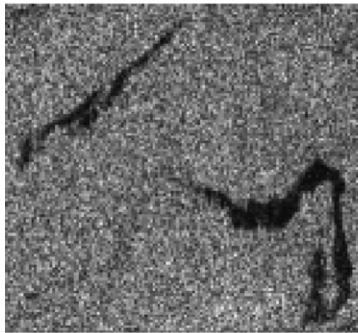
b) Detection of well-defined natural phenomena on a bright background

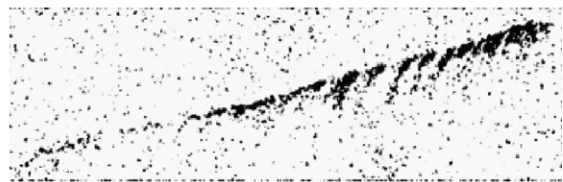c) Detection of a very fresh oil spill without clear borders on a bright background

Fig. 2. Three different examples of MLP141 network classification. a) Detection of a well-defined old oil spill on a dark background. b) Detection of well-defined natural phenomena on a bright background. c) Detection of a very fresh oil spill without clear borders on a bright background.

Fig. 2 contains three classification results using the MLP1:4:1 network. In the first two cases, an oil spill and a look-alike are presented. Both have very clear borders with the sea surface and have been successfully detected. The first example with the oil spill is one of the easy cases where the borders of the dark feature are very clear, the background area has a uniform brighter texture and the dark feature is not broken in pieces. Such cases are quite easy to be detected and classified as oil spills. The second example (Fig. 2b) contains two look-alikes, which have same characteristics with oil spills. For the dark detection step the natural phenomena can be detected quite easy as they are well defined black areas, united, in a relative bright background. Some very small dark areas that are also detected, will be classified as not oil spill in the discrimination process because of their small size. For these two look-alikes the classification step is the most important, as they are presented

quite similar to oil spills. Nevertheless, the proposed vector of 10 features in combination with the neural network knowledge can classify them as look-alikes. The last example (Fig. 2c) contains a case of an oil spill where the borders between the dark object and the sea were not very well defined. This case is one of the most difficult both in terms of dark feature detection and oil spill classification. The oil spill is very fresh, is presented on a bright background, it has not yet been affected by spreading and it has broken in several pieces probably due to Langmuir circulations (i.e. formation of cells of rotating water that parallel the surface due to wind and to currents). In this case the neural network can detect the main dark formation but also produce a quite high amount of noise that decreases the overall detection capability. In similar cases with fresh and linear oil spills not yet affected by spreading the detection part is getting very difficult. Because of not correct dark object detection

Table 1
Accuracy matrix (Congalton and Green, 1998) for the oil spill and look-alike discrimination

Khat = 0.79	Look alike	Oil spill	User's (%)
Look alike	39	3	92.86
Oil spill	6	31	83.78
Producer's (%)	86.67	91.18	88.61

when the classification takes part the discrimination between oil spills and look-alikes is very difficult. In this case the bigger part of the oil spill in the right part of the image was classified successfully as oil spill but the rest classified as look-alike. This specific case was misclassified by the second neural network.

Regarding the discrimination between oil spills and look-alikes, the MLP10:51:2 network resulted in 89% overall testing accuracy with 0.79 K-Hat statistic (Congalton and Green, 1998) and 92% g-mean statistic (Kubat et al., 1998). In Table 1 the accuracy matrix (Congalton and Green, 1998) of the overall data can be seen. From the 34 oil spills contained in the test set only three were misclassified to look-alikes, i.e. the results had an accuracy of 91%, and for the 45 look-alikes of the set 6 misclassified as oil spills, i.e. 87% accuracy.

5. Conclusion — Discussion

A combination of two neural networks has been successfully used for dark formation detection and for oil spill and look-alike discrimination using high resolution SAR images. Dark formations were detected with an accuracy of 94% and oil spills were separated successfully from look-alikes for 89% of the cases. In real world these accuracies can vary. Our data set contains a limited balanced number of examples while usually SAR images contain a large number of look-alikes and few oil spills. In a real world scenario a new assessment about the method's accuracy should be given.

Five issues have to be faced (Kubat et al., 1998) while dealing with oil spill detection problem in machine learning domain: the way examples are presented, imbalance of the dataset's class distribution, validity of the data selection, feature engineering problem and highly dynamic environment. In this study, as the number of the oil spills samples was in balance with the number of look-alikes samples, all the examples were combined into one large dataset. Also the training and testing set was totally separated. With this tactic we were able to calculate easily the classifier accuracy and avoid the problems of small disjunctions (Kubat et al., 1998) and domination due to the large number of examples in one class. The next issue was the imbalance of the dataset's class distribution i.e. many look-alikes and few oil

spill samples. In the present study the dataset was balanced between look-alikes and oil spills samples. Thus, there was no need to find ways to balance the dataset and to use specific training algorithms. Moreover, except the images containing both oil spills and look-alikes we used images containing only look-alikes resulting in a dataset with large variety on look-alikes and oil spills. In combination with the fact that look-alikes are natural phenomena whose presence in an image is independent of the presence of an oil spill we have confidence to the validity of our data selection. The feature engineering problem i.e. how many and which features should be used to distinguish oil spills from look-alikes was examined extensively in a previous study (Stathakis et al., 2006). The used combination of ten features has been found optimum for the discrimination between oil spills and look-alikes. Last but not the least, the problem of working in highly dynamic environment i.e. the change of several factors (e.g. image dataset, low level processing, learning algorithms) was faced at the beginning of the experiment adopting a clear and stable protocol. Thus, dataset, features and training algorithm were stable for the whole procedure.

While it is inappropriate to compare different methodologies without using exactly the same data set a reference with previous work can be given. The neural classification proposed by Del Frate et al. (2000) presents accuracy of 82% for real oil spills and 90% as look-alikes. The statistical model of Solberg et al. (1999) presents accuracy of 94% of oil slicks and 99% for the look-alikes. The probabilistic method of Fiscella et al. (2000) presents overall accuracy close to 80%, while those from Nirchio et al. (2005) presents overall accuracy close to 90%.

Neural network's ability to handle successfully non-linearly separable classes is a big advantage against the commonly used statistical approaches. The proposed methodology works satisfactorily in several difficult oil spill detection cases, independent from sea-state conditions and the original SAR data quality (sensor calibration status, speckle, atmospheric conditions etc.). Further research could include more images, other network categories and variations of the existing networks.

References

Alpers, W., Wismann, V., Theis, R., Huhnerfuss, H., Bartsch, N., Moreira, J., Lyden, J., 1991. The damping of ocean surface waves by monomolecular sea slicks measured by airborne multi-frequency radars during the saxon-fpn experiment. Proc. International Geoscience and Remote Sensing Symposium (IGARSS91), Helsinki, Finland, pp. 1987–1990.

Benelli, G., Garzelli, A., 1999. Oil-Spills Detection in SAR Images by Fractal Dimension Estimation. Proc. International Geoscience and Remote Sensing Symposium (IGARSS 99) Hamburg, Germany, pp. 218–220.

Bishop, C., 1995. Neural Networks for Pattern Recognition. Oxford University Press, Oxford.

Brekke, C., Solberg, A., 2005. Feature Extraction for Oil Spill Detection Based on SAR Images. Lecture notes in computer science, vol. 3540/2005, pp. 75–84. doi:10.1007/b137285.

Calabressi, G., Del Frate, F., Lichtenegger, J., Petrocchi, A., 1999. Neural Networks for the oil spill detection using ERS-SAR data. Proc. International Geoscience and Remote Sensing Symposium (IGARSS 99), Hamburg, Germany, pp. 215–217.

Congalton, R., Green, K., 1998. Assessing the Accuracy of Remotely Sensed Data: Principles and Practices. Lewis Publishers.

Del Frate, F., Petrocchi, A., Lichtenegger, J., Calabresi, G., 2000. Neural networks for oil spill detection using ERS-SAR data. IEEE Transactions on Geoscience and Remote Sensing 38 (5), 2282–2287.

Espedal, H.A., Johannessen, J.A., 2000. Detection of oil spills near offshore installations using synthetic aperture radar (SAR). International Journal of Remote Sensing 21 (11), 2141–2144.

Espedal, H.A., Wahl, T., 1999. Satellite SAR oil spill detection using wind history information. International Journal of Remote Sensing 20 (1), 49–65.

Fiscella, B., Giancaspro, A., Nirchio, F., Pavese, P., Trivero, P., 2000. Oil spill detection using marine SAR images. International Journal of Remote Sensing 21 (18), 3561–3566.

Gade, M., Scholz, J., Viebahn, C., 2000. On the delectability of marine oil pollution in European marginal waters by means of ERS SAR imagery. Proc. International Geoscience and Remote Sensing Symposium (IGARSS 2000), Honolulu Hawaii, VI, pp. 2510–2512.

Haralick, R.M., 1979. Statistical and structural approaches to texture. In: Proceedings of the IEEE, vol. 67 (5), pp. 786–804.

Hovland, H.A., Johannessen, J.A., Digranes, G., 1994. Slick detection in SAR images. Proc. International Geoscience and Remote Sensing Symposium (IGARSS 94), Pasadena CA, USA, pp. 2038–2040.

Kanellopoulos, I., Wilkinson, G., 1997. Strategies and best practice for neural network image classification. International Journal of Remote Sensing 18 (4), 711–725.

Karathanassi, V., Topouzelis, K., Pavlakis, P., Rokos, D., 2006. An object-oriented methodology to detect oil spills. International Journal of Remote Sensing 27 (23), 5235–5251.

Kavzoglu, T., Mather, P., 2003. The use of backpropagation artificial neural network in land cover classification. International Journal of Remote Sensing 24 (23), 4907–4938.

Keramitsoglou, I., Cartalis, C., Kiranoudis, C., 2002. An integrated fuzzy classification system for automatic oil spill detection using SAR images. In: Bostater, C.R., Santoleri, R. (Eds.), Proc. of SPIE-Volume 4880 Remote Sensing of the Ocean and Sea Ice 2002, 23–27 September 1999, Creta, Greece, pp. 131–140.

Kubat, M., Holte, R.C., Matwin, S., 1998. Machine learning for the detection of oil spills in satellite radar images. Machine Learning 30 (2–3), 195–215.

Lichtenegger, J., Calabresi, G., Petrocchi, A., 2000. A near-real time oil slick monitoring demonstrator for the Mediterranean. XIX ISPRS Congress, Amsterdam, The Netherlands, XXXIII, pp. 193–200.

Lu, J., Lim, H., Liew, S., Bao, M., Knowoh, L., 1999. Ocean oil pollution mapping with ERS synthetic aperture radar imagery.

International Geoscience and Remote Sensing Symposium (IGARSS99), Hamburg, Germany, pp. 212–214.

Martinez, A., Moreno, V., 1996. An oil spill monitoring system based on SAR images. Spill Science and Technology Bulletin 3 (1–2), 65–71.

Nirchio, F., Sorgente, M., Giancaspro, A., Biamino, W., Parisato, E., Ravera, R., Trivero, P., 2005. Automatic detection of oil spills from SAR images. International Journal of Remote Sensing 26 (6), 1157–1174.

Pavlakis, P., 2001. On the monitoring of illicit vessel discharges using spaceborne sar remote sensing; a reconnaissance study in the Mediterranean Sea. Annals of Telecommunication 56 (11–12), 1–19.

Pavlakis, P., Tarchi, D., Sieber, A., 2001. On the Monitoring of Illicit Vessel Discharges. A Reconnaissance Study in the Mediterranean Sea. European Commission, EUR 19906 EN.

Rio, J.N., Lozano-García, F.D., 2000. Spatial filtering of radar data (RADARSAT) for wetlands (Brackish Marshes) classification. Remote Sensing of Environment 73 (2), 143–151.

Rumelhart, E.D., McClelland, J., 1986. PDP models and general issues in cognitive science. In: Rumelhart, D.E., McClelland, J.L. (Eds.), Parallel Distributed Processing. MIT Press, pp. 110–146.

Solberg, R., Theophilopoulos, N.A., 1997. Envisys — a solution for automatic oil spill detection in the Mediterranean. 4th International Conference on Remote Sensing for Marine and Coastal Environments, Orlando, Florida, 17–19 March 1997, pp. 3–12.

Solberg, A., Storvik, G., Solberg, R., Volden, E., 1999. Automatic detection of oil spills in ERS SAR images. IEEE Transactions on Geocience and Remote Sensing 37 (4), 1916–1924.

Stathakis, D., Topouzelis, K., Karathanassi, V., 2006. Oil spill detection using evolved neural networks. In: Bruzzone, L. (Ed.), Proc. of SPIE Volume 6365- Image and Signal Processing for Remote Sensing XII, Stockholm, Sweden, 11–14 September. 9 pages.

Topouzelis, K., Karathanassi, V., Pavlakis, P., Rokos, D., 2002. Oil spill detection: SAR multi-scale segmentation and object features evaluation. In: Bostater, C.R., Santoleri, R. (Eds.), Proc. of SPIE-Volume 4880 Remote Sensing of the Ocean and Sea Ice 2002, 23–27 September 1999, Creta, Greece, pp. 77–87.

Topouzelis, K., Karathanassi, V., Pavlakis, P., Rokos, D., 2003. A neural network approach to oil spill detection using SAR data. 54th International Astronautical Congress, Bremen, Germany, 29.Sept-03.Oct (on CDROM).

Topouzelis, K., Karathanassi, V., Pavlakis, P., Rokos, D., 2004. Oil Spill Detection Using RBF Neural Networks and SAR Data. XX. ISPRS Congress, Istanbul, 12–23 July. 6 p. (on CDROM).

Topouzelis, K., Karathanassi, V., Pavlakis, P., Rokos, D., 2006. Dark formation detection using recurrent neural networks and SAR data. In: Bruzzone, L. (Ed.), Proc. of SPIE- Volume 6365 Image and Signal Processing for Remote Sensing, Stockholm, Sweden, 11–14 September.

Topouzelis, K., Karathanassi, V., Pavlakis, P., Rokos, D., in press. Dark formation detection using neural networks. International Journal of Remote Sensing.

Ziemke, T., 1996. Radar image segmentation using recurrent artificial neural networks. Pattern Recognition Letters 17 (4), 319–334.